Acta Crystallographica Section D
Biological Crystallography
ISSN 1399-0047

Structure of the nisin leader peptidase NisP revealing a C-terminal autocleavage activity

Yueyang Xu,[a]‡ Xin Li,[a]‡ Ruiqing Li,[a] Shanshan Li,[a] Hongqian Ni,[a] Hui Wang,[a] Haijin Xu,[a] Weihong Zhou,[a] Per E. J. Saris,[b] Wen Yang,[a]* Mingqiang Qiao[a]* and Zihe Rao[a]

[a]State Key Laboratory of Medicinal Chemical Biology, College of Life Sciences, Nankai University, Tianjin, People's Republic of China, and [b]Department of Applied Chemistry and Microbiology, Division of Microbiology, University of Helsinki, Helsinki, Finland

‡ These two authors contributed equally to this work.

Correspondence e-mail: yangwen05@gmail.com, mingqiangqiao@aliyun.com

Received 9 November 2013
Accepted 24 February 2014

PDB reference: NisP, 4mzd

Nisin is a widely used antibacterial lantibiotic polypeptide produced by *Lactococcus lactis*. NisP belongs to the subtilase family and functions in the last step of nisin maturation as the leader-peptide peptidase. Deletion of the *nisP* gene in LAC71 results in the production of a non-active precursor peptide with the leader peptide unremoved. Here, the 1.1 Å resolution crystal structure of NisP is reported. The structure shows similarity to other subtilases, which can bind varying numbers of Ca atoms. However, no calcium was found in this NisP structure, and the predicted calcium-chelating residues were placed so as to not allow NisP to bind a calcium ion in this conformation. Interestingly, a short peptide corresponding to its own 635–647 sequence was found to bind to the active site of NisP. Biochemical assays and native mass-spectrometric analysis confirmed that NisP possesses an auto-cleavage site between residues Arg647 and Ser648. Further, it was shown that NisP mutated at the auto-cleavage site (R647P/S648P) had full catalytic activity for nisin leader-peptide cleavage, although the C-terminal region of NisP was no longer cleaved. Expressing this mutant in *L. lactis* LAC71 did not affect the production of nisin but did decrease the proliferation rate of the bacteria, suggesting the biological significance of the C-terminal auto-cleavage of NisP.

1. Introduction

Nisin is a natural antibacterial polypeptide produced by *Lactococcus lactis*. It belongs to the lantibiotics and consists of 34 residues. Nisin effectively inhibits the growth of a broad range of Gram-positive bacteria (Hurst, 1981; Delves-Broughton, 1990). As it is nontoxic in mammals, nisin has been widely used as a food preservative in a variety of products around the world (Delves-Broughton *et al.*, 1996). Nisin biosynthesis-related genes are organized into the *nisABTCIPRK*, *nisI*, *nisRK* and *nisFEG* operons (Ra *et al.*, 1996; Li & O'Sullivan, 2006). Nisin is synthesized as an inactive prepeptide composed of 57 residues, followed by two modification steps consisting of dehydration reactions and ring formation performed by NisB and NisC, respectively. After transport across the cytoplasmic membrane by NisT, the final step in nisin maturation is the proteolytic cleavage of the first 23 amino-terminal residues by NisP (Kuipers *et al.*, 1993). Disruption of the *nisP* gene leads to an inability to cleave the nisin leader peptide (Qiao *et al.*, 1996) and the secreted nisin precursor shows no significant antimicrobial activity (van der Meer *et al.*, 1993; Koponen *et al.*, 2002).

NisP (UniProt accession code D9IXC0) belongs to the subtilase family of serine proteases (Pfam entry Peptidase_S8) and has been predicted to interact with calcium ions (Siezen

Table 1
Data-collection and refinement statistics.

Values in parentheses are for the highest resolution shell.

Data-collection statistics	
Wavelength (Å)	0.9798
Space group	$P2_1$
Unit-cell parameters (Å, °)	a = 49.89, b = 44.97, c = 74.65, β = 106.82
Resolution (Å)	50–1.10 (1.14–1.10)
$\langle I/\sigma(I)\rangle$	38.7 (2.4)
Completeness (%)	98.4 (95.8)
Average multiplicity	6.8 (4.4)
$R_{\rm merge}$†	0.078 (0.448)
Structure-refinement statistics	
Resolution (Å)	50–1.10
Average B factor (Å^2)	10.3
$R_{\rm work}/R_{\rm free}$‡	0.138/0.160
Wilson B factor (Å^2)	10.56
R.m.s. deviation from ideal bond lengths§ (Å)	0.014
R.m.s. deviation from ideal bond angles§ (°)	1.47
Ramachandran favoured (%)	97.6
Ramachandran outliers (%)	0.0
Poor rotamers (%)	0
Clashscore	5

† $R_{\rm merge} = \sum_{hkl}\sum_i |I_i(hkl) - \langle I(hkl)\rangle|/\sum_{hkl}\sum_i I_i(hkl)$, where $I_i(hkl)$ is an individual intensity measurement and $\langle I(hkl)\rangle$ is the average intensity for all reflections. ‡ $R_{\rm work}/R_{\rm free} = \sum_{hkl}||F_{\rm obs}| - |F_{\rm calc}||/\sum_{hkl}|F_{\rm obs}|$, where $F_{\rm obs}$ and $F_{\rm calc}$ are the observed and calculated structure factors, respectively. § Ideal values are derived from Engh & Huber (1991).

et al., 1995). Like most subtilases, NisP is synthesized as a pre-pro-enzyme of 682 residues, and the N-terminal 22 residues constitute a Sec-signal sequence which is needed for secretion of NisP from the cell (Lubelski *et al.*, 2008). The propeptide sequence stretches up to residue 195 (Lubelski *et al.*, 2008) and has been reported to be auto-removed by NisP itself, leading to the formation of mature NisP (Power *et al.*, 1986; Germain *et al.*, 1992; Leduc *et al.*, 1992; Lubelski *et al.*, 2008). In addition, NisP has a long C-terminal extension, possessing a Gram-positive cell-wall anchor consensus motif LP*X*TG*X* (residues 652–657; van der Meer *et al.*, 1993) and a spacer region of 100 residues (residues 550–651) of unclear function (Sahl & Bierbaum, 1998; McAuliffe *et al.*, 2001). To better understand the molecular architecture of NisP, we determined the 1.1 Å resolution crystal structure of the major part of mature NisP (residues 224–566), which shares strong similarity with other subtilases but lacks calcium ion-binding sites. Interestingly, a short C-terminal peptide (residues 635–647) was discovered to bind near the catalytic triad in the surface cleft of NisP, hinting at a C-terminal auto-cleavage activity. Using biochemical assays and native mass-spectrometric analysis, we verified this C-terminal auto-cleavage activity and provided evidence of a link between the auto-cleavage activity and the proliferation rate of *L. lactis*.

2. Experimental procedures

2.1. Plasmid construction

Full-length and truncated *nisP* genes were amplified from the genome of *L. lactis* strain N8. The PCR product was purified and digested with *Bam*HI and *Xho*I. For crystallization and the *in vitro* enzyme-activity assay, digested PCR products encoding mature NisP were cloned into the pET-32a vector (Invitrogen). For the Western blot assay, a gene fragment for mature NisP with an additional C-terminal 6×His tag was amplified and constructed in pGEX-6p-1 (Invitrogen). *Escherichia coli* DH5α and BL21 (DE3) (Novagen) were used as recipient strains in the cloning and expression experiments. For expression of NisP in *L. lactis*, pLEV16 (Xuanyuan *et al.*, 2010) carrying the full-length *nisP* gene was used as the expression vector in the *nisP* mutant strain LAC71 (Qiao *et al.*, 1996).

2.2. Protein expression and purification

The *E. coli* strains were grown in Luria–Bertani broth medium containing 100 µg ml^{-1} ampicillin at 37°C. When the OD_{600} of the culture reached 0.6, isopropyl β-D-1-thiogalactopyranoside was added to the growth medium to a final concentration of 0.5 m*M* to induce the expression of recombinant proteins. The induced cultures were grown at 16°C for 16 h. The cells were harvested by centrifugation, resuspended in phosphate-buffered saline (1× PBS pH 7.4) and then lysed by sonication on ice. The cell debris was removed by centrifugation at 18 000*g* for 40 min at 4°C. The supernatant was loaded onto an Ni–NTA column (GE Healthcare) equilibrated with 1× PBS. The column was washed briefly with 1× PBS and then extensively with wash buffer (1× PBS, 20 m*M* imidazole). The target protein was eluted with 1× PBS containing 300 m*M* imidazole. The eluted NisP protein was buffer-exchanged to 1× PBS by overnight dialysis and finally concentrated to approximately 20 mg ml^{-1}. The protein was kept at 4°C for 12 h in the presence of 0.2 mg ml^{-1} thrombin and reapplied onto an Ni–NTA column to remove the tag. The protein was concentrated and applied onto a Superdex 75 column (GE Healthcare) equilibrated with 1× PBS and was further purified using anion-exchange chromatography on a Resource Q column (GE Healthcare). The purified protein was finally exchanged into a buffer consisting of 20 m*M* Tris pH 8.0, 100 m*M* NaCl for crystallization.

Selenomethionine (SeMet)-labelled protein was expressed using the methionine-auxotrophic *E. coli* strain B834 (DE3) (Novagen) in M9 minimal medium supplemented with 50 mg selenomethionine per litre. The selenomethionine-labelled protein was purified using the same method as used for the wild-type NisP protein.

2.3. Crystallization, data collection and structure determination

The purified mature NisP protein was concentrated to 20 mg ml^{-1}. Initial crystallization screening by the sitting-drop vapour-diffusion method was performed at 20°C using Crystal Screen kits (Hampton Research). Thin plate-shaped crystals were observed after four weeks. These crystals diffracted poorly and were not suitable for structure determination. After optimization using the hanging-drop vapour-diffusion method, diffraction-quality crystals were obtained using a reservoir consisting of 0.1 *M* HEPES pH 7.5, 24–32% 1,4-dioxane. Crystals of selenomethionine-labelled protein were

obtained from the same condition. The crystals were briefly soaked in a cryoprotectant solution consisting of 20% glycerol in the mother liquor and flash-cooled in liquid nitrogen prior to data collection.

Data for the selenomethionine-derivative crystal were collected at 100 K on beamline BL-5A at the Photon Factory synchrotron facility (KEK, Tsukuba, Japan). All diffraction data were integrated, scaled and merged using the *HKL*-2000 suite (Otwinowski & Minor, 1997). The structure of mature NisP was solved by *PHENIX* (Adams *et al.*, 2010) using the single-wavelength anomalous dispersion method. The initial NisP model was built using *ARP*/*wARP* (Perrakis *et al.*, 1999). *Coot* (Emsley *et al.*, 2010) was used for further model rebuilding, and the structure was refined with *REFMAC*5 (Murshudov *et al.*, 2011) in the *CCP*4 suite (Winn *et al.*, 2011) and *PHENIX*. The data-collection, structure-determination and refinement statistics are summarized in Table 1. The coordinates of the crystal structure of NisP have been deposited in the Protein Data Bank (http://www.pdb.org; Berman *et al.*, 2000) with accession code 4mzd. All structural figures were created using *PyMOL* (v.1.3r1; Schrödinger).

2.4. Enzyme-activity assay

For the *in vitro* enzyme digestion activity assay, the fluorescent substrate peptide edans-EGAVSVRSQEIK-dabcyl was synthesized. In the peptide, the quencher 4-(dimethylaminoazo)benzene-4-carboxylic acid (dabcyl) efficiently quenches the fluorophore 5-[(2-aminoethyl)amino]naphthalene-1-sulfonic acid (edans). When the peptide is internally cleaved, the fluorophore edans can be excited by 340 nm light, with fluorescence emission at 485 nm. The enzyme activity was analysed by detecting the fluorescence emission level. Stock solutions were prepared by dissolving 10 mg in 100 µl DMSO. The reaction mixture (100 µl) was as follows: 20 m*M* Tris pH 8.5, 150 m*M* NaCl, 0.5% Triton X-100, 0.1% DMSO, 0.05 µg µl^{-1} substrate and 0.001 µg µl^{-1} enzyme. Changes in the fluorescence values were detected using a microplate reader.

For the bacterial inhibition assay, lawns of nisin-sensitive indicator bacteria (*Micrococcus luteus* A1 NCIMB86166) were prepared. LAC71 is a *nisP*-deleted strain expressing the nisin precursor peptide, to which the leader peptide is still attached (Qiao *et al.*, 1996). When performing the assay with purified proteins, 150 µl culture supernatant of LAC71 was mixed with purified wild-type or mutant mature NisP protein and added to the bacterial lawn. For the *in vivo* condition, the pLEV16 plasmid carrying the full-length wild-type or mutant *nisP* gene was electrotransformed into LAC71. The transformants were identified and cultured in M17GS broth (4.23% M17, 0.5% glucose, 0.55% sucrose). Next, 40 µl culture supernatant was added to the bacterial lawn. The lawns were placed at 37°C to allow bacterial proliferation and inhibition-zone formation.

For the Western blot, aliquots of *E. coli* BL21 (DE3) cultures expressing both the GST tag and the 6×His tag attached to wild-type or mutant mature NisP were taken and the tags were sequentially detected using 6×His-tag and GST-tag antibodies.

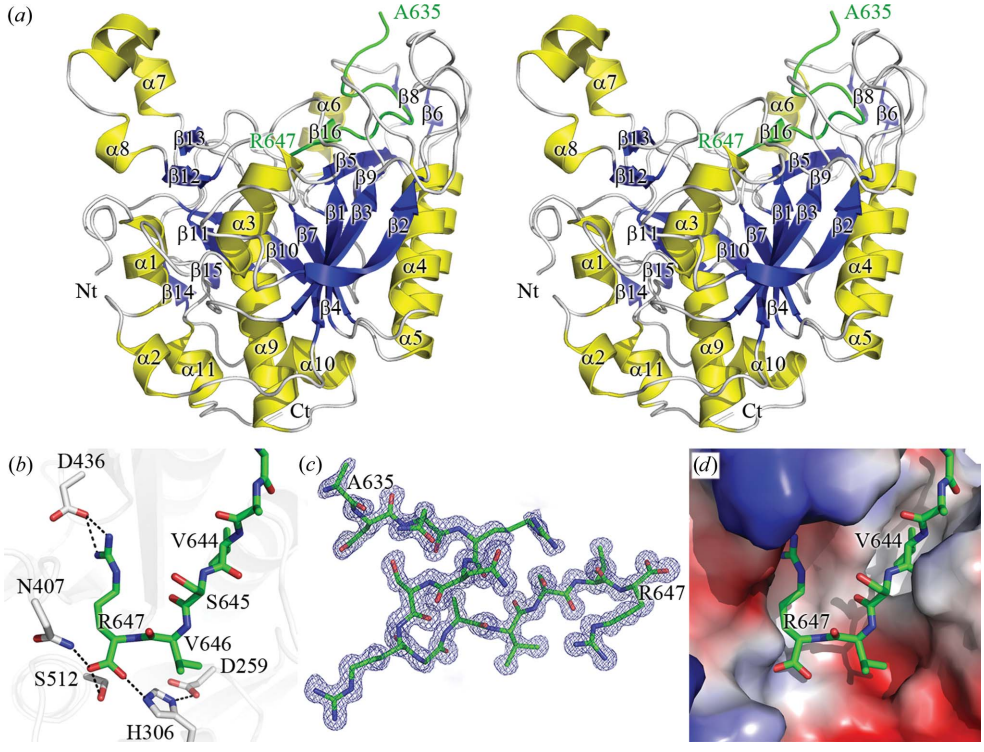

Figure 1
Structure of mature NisP. (*a*) Stereo ribbon diagram. Secondary structures are coloured yellow (helices), blue (strands) and white (loops). The C-peptide (residues 635–647) is coloured green. (*b*) Interactions at the interface between the C-peptide (green) and residues in the active site (grey). Salt bridges and hydrogen bonds are indicated by dashed lines. (*c*) The $2mF_o - DF_c$ density of the bound C-peptide contoured at ∼0.35 e Å^{-3}. (*d*) Charge-potential illustration of NisP with the bound C-peptide shown as green sticks.

3. Results

3.1. Structure determination and overall structure

The SeMet-derivative mature NisP structure was determined at 1.10 Å resolution (PDB entry 4mzd) using the single-wavelength anomalous diffraction method. The crystal belonged to space group $P2_1$ with one mature NisP protein molecule and 454 ordered water molecules in the asymmetric unit. The model was refined to a final working *R* factor of 13.8% and a free *R* factor of 16.0%. The Ramachandran plot calculated by *MolProbity* (Chen *et al.*, 2010) showed that 97.6% of the residues have their main-

chain torsion angles in the most favourable region, and no residues lie in the disallowed region. The final structure contains the majority (residues 224–566) of the mature protein and a short peptide from the C-terminus (residues 635–647, termed the C-peptide). Residues 196–223, 567–634 and 648–682 were not visualized in the final model owing to cleavage and degradation in the crystallization process (Supplementary Fig. S1[1]). The detailed statistics are provided in Table 1.

The NisP structure has a heart-like shape with an open cleft on the surface. The residues form 11 α-helices (α1–α11) and 16 β-strands (β1–β16), as shown in Fig. 1(*a*). Helices α3, α9 and a large curved parallel β-sheet composed of strands β2, β3, β1, β4, β7, β10 and β11 are in the central part. Helices α1, α2 and α11 and β-strands β15 and β14 are also localized on the same side and adjacent to helices α3 and α9, while the outer helices α4 and α5 are on the other side of the large central β-sheet. Helices α6, α7 and α8 and strands β6 and β8 stretch outwards above the entire structure and facilitate the formation of the open cleft, along with some stretched loops (Fig. 1*a*). The cleft is capable of accommodating several amino-acid residues and may take part in substrate recognition and binding.

Mature NisP has a similar structure to other subtilases (Siezen *et al.*, 1995), *e.g.* epidermin leader peptide-processing serine protease (EpiP; PDB entry 3qfh; r.m.s. deviation of 1.8 Å for 333 residues; Center for Structural Genomics of Infectious Diseases, unpublished work), thermitase (PDB code 1tec; r.m.s. deviation of 1.4 Å for 262 residues; Gros et al., 1991), Tk-subtilisin (PDB entry 2z2z; r.m.s. deviation of 1.8 Å for 265 residues; Tanaka *et al.*, 2007) and subtilisin BPN′ (PDB entry 1lw6; r.m.s. deviation of 1.9 Å for 264 residues; Radisky & Koshland, 2002).

3.2. Active site and C-peptide

The active site and catalytic mechanism of subtilases have been thoroughly discussed in previous studies (Dodson & Wlodawer, 1998; Polgar, 2005). According to sequence alignment with these well characterized subtilases, the active site of NisP consists of the catalytic triad residues Asp259, His306 and Ser512, which are totally conserved in the subtilase family (Supplementary Fig. S2; Siezen *et al.*, 1991). Asp259 lies on strand β1 at the C-terminus. His306 and Ser512 are located at the N-termini of helices α3 and α9, respectively. Among the triad, the O^{γ} atom of Ser512 is 3.06 Å from the $N^{\varepsilon 2}$ atom of His306, and the $N^{\delta 1}$ atom of His306 is 2.67 Å from the $O^{\delta 2}$ atom of Asp259 (Fig. 1*b*), suggesting hydrogen bonds between the residues that contribute to the stabilization of the catalytic site.

Around the open cleft area, additional distinct density could be observed apart from the catalytic core. A short peptide was built in with the sequence ANNRNSRGAVSVR, which corresponds to the C-terminal 635–647 region (C-peptide) of NisP (Fig. 1*c*). In the C-peptide, the residues Ser645 and Val646 form a small β-strand (β16) and join in the antiparallel β-sheet composed of β5 and β9. The hydrophobic residues Ala643, Val644 and Val646 of the C-peptide interact with Phe286, Met304, Val334, Phe335, Leu339, Val345, Ile362 and Tyr387, forming a hydrophobic pocket. The side chain of Arg647 is recognized by Asp436 through a charge interaction, and the terminal carboxyl group is stabilized by Ser512 and His306 through hydrogen bonds (Fig. 1*b*). Additional hydrogen bonds can also be identified between the residue pairs Ser340/Val644, Asp376/Arg641, Thr378/Arg641, Arg426/Asn639 and Phe425/Asn637 that help to stabilize the C-peptide (Fig. 1*b*). At the C-terminus of the C-peptide, the electron density ends abruptly at the main-chain carboxyl group of Arg647. As this arginine residue is located exactly at the catalytic triad, we propose that the C-terminus (648–682) of the mature NisP is auto-cleaved at this site. Because this hypothetical auto-cleavage site lies at the C-terminus of the catalytic domain, and to distinguish it from the N-terminal auto-cleavage of NisP during maturation, we term this auto-cleavage the C-terminal auto-cleavage.

3.3. Verification of the C-terminal auto-cleavage activity

To confirm whether NisP can recognize its own sequence near the C-terminus as a substrate, we first synthesized fluorescent and quenching group-labelled polypeptide with a sequence corresponding to the putative C-terminal cleavage site (sequence: edans-EGAVSVRSQEIK-dabcyl) and performed an *in vitro* enzyme-digestion assay. As expected,

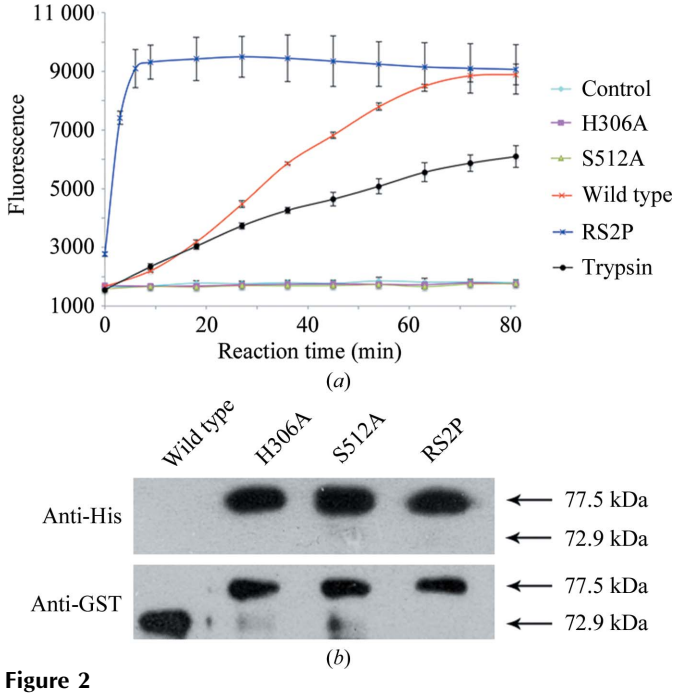

Figure 2
Enzymatic activity of various mutations of NisP. (*a*) Activity assays using the purified wild-type NisP or mutant enzyme and the fluorescent peptide substrate edans-EGAVSVRSQEIK-dabcyl. Fluorescence values were measured every 9 min and are shown as curves with different colours and symbols. (*b*) Auto-cleavage activity assay. GST and 6×His tags were both added to wild-type or mutant mature NisP. Anti-6×His-tag and anti-GST-tag antibodies were used to detect the tags. The values 77.5 and 72.9 kDa refer to the molecular weight of NisP with the C-terminus intact and cleaved off, respectively.

[1] Supporting information has been deposited in the IUCr electronic archive (Reference: KW5085).

the fluorescence value increased substantially when the synthesized polypeptide and the wild-type mature NisP protein were mixed, indicating digestion of the polypeptide. In contrast, neither of the active-site mutants (H306A and S512A) of mature NisP showed any cleavage activity towards the polypeptide (Fig. 2*a*). These results demonstrated that NisP is capable of recognizing and cleaving the sequence of the hypothetical C-terminal auto-cleavage site.

Based on the *in vitro* assay results, we then verified the C-terminal auto-cleavage activity of NisP. For this purpose, a GST tag and a 6×His tag were added to the N-terminus and the C-terminus of mature NisP, respectively. As expected, the N-terminal GST tag of the double-tagged wild-type mature NisP was detected well by anti-GST antibodies in the Western blot experiments, but the C-terminal 6×His tag could not be detected using anti-6×His antibodies, suggesting that it was not present (Fig. 2*b*). To eliminate the possibility that the C-terminus was being removed by other *E. coli* enzymes, the same Western blot experiments were performed on active-site mutated (H306A or S512A) double-tagged mature NisP. For each mutant, both the GST tag and the 6×His tag were detectable, indicating that the C-terminus was intact. These results confirmed that NisP possesses C-terminal auto-cleavage activity.

To further identify the C-terminal auto-cleavage site, we designed an R647P/S648P double mutant (RS2P). As the enzymatic hydrolysis of the peptide bond between two proline residues normally requires a class of special proteases such as the prolidases (Cunningham & O'Connor, 1997), the peptide linkage between Pro647 and Pro648 in the NisP RS2P mutant should not be auto-cleaved by the mutant. In the Western blot experiments on the purified double-tagged RS2P mutant, both the GST tag and the 6×His tag were detected, as shown in Fig. 2(*b*), confirming that the Arg647/Ser648 site is the exact and the only C-terminal auto-cleavage site of NisP. Meanwhile, purified double-tagged wild-type and mutated NisP proteins were assayed by native protein mass spectrometry. The molecular-weight differences calculated by MS also verified cleavage after Arg647 (Supplementary Fig. S3).

To further explore whether the C-terminus of NisP could affect the enzyme activity, purified RS2P mutant protein (without the tags) was mixed with the synthetic polypeptide substrate. As in the wild-type NisP protein, a remarkable increase in fluorescence was observed (Fig. 2*a*), indicating that the mutant can still cleave the synthetic polypeptide effectively. Notably, the RS2P mutant presented significantly higher activity than the wild-type NisP (Fig. 2*a*). Moreover, the same amount of purified wild-type mature NisP, S512A mutant or RS2P mutant protein was applied to the bacterial inhibition assay using the supernatant of the LAC71 strain culture as the source of prenisin. On the bacterial lawn, the S512A mutant barely produced any bacterial inhibition ring, while both the wild type and the RS2P mutant generated clear bacterial inhibition zones of approximately the same size (Fig. 3*a*). This experiment suggests that the wild-type NisP and the RS2P mutant have approximately identical nisin maturation activities.

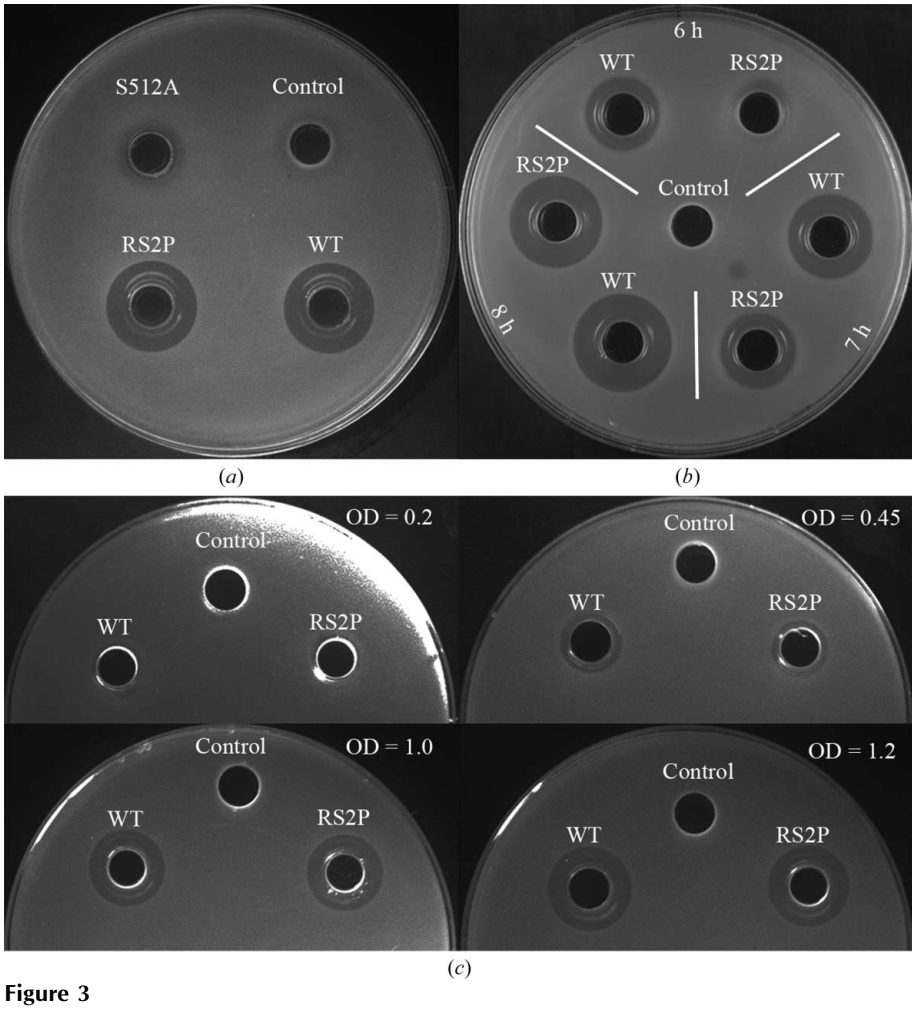

Figure 3
Bacterial inhibition assays on the lawns of nisin-sensitive indicator bacteria. (*a*) Bacterial inhibition assay performed with the purified protein. 150 µl culture supernatant of the LAC71 strain was mixed with 0.01 µg wild-type or RS2P mutant mature NisP protein or buffer (control) before application to a lawn. (*b*, *c*) Bacterial inhibition assay for intact LAC71 strain containing pLEV16-*nisP*, pLEV16-*nisP-RS2P* recombinant plasmid or only the pLEV16 vector (control). Aliquots of the cultures were taken at different time points (*b*) or OD_{600} value points (*c*), and 40 µl of the culture supernatant was added to each well.

3.4. Cleavage of the NisP C-terminus affects *L. lactis* proliferation

The results above show that NisP is capable of removing its own C-terminus,

and that the removable C-terminus does not affect the activity of NisP. To explore the biological significance of the C-terminal auto-cleavage activity, we inserted the full-length (residues 1–682) NisP gene or the full-length RS2P mutant gene into the *L. lactis* expression vector pLEV16 and transformed the recombinant plasmids into the *nisP* mutated *L. lactis* strain LAC71. Bacteria containing each of the two plasmids were cultured. Aliquots of each culture were taken at different culture times, and the supernatants were applied to bacterial inhibition assays. Both cultures exhibited antibacterial capability, and the sizes of the bacterial inhibition zones increased dramatically over time. However, the zones for the wild-type NisP expression culture were always larger than those for the RS2P mutant expression culture (Fig. 3*b*). These results seem to imply higher nisin production for the wild-type NisP expression culture.

As we have shown that the activities of the wild-type NisP and the RS2P mutant are approximately identical in the maturation of nisin, the higher nisin production of the wild-type NisP expression culture appears not to be linked to the catalytic activities of the enzyme derivatives. We examined the cultures themselves and observed that the strain expressing the RS2P mutant grew more slowly than the strain expressing the wild-type NisP. The optical density at 600 nm (OD_{600}) of the two cultures was measured at different time points. In the testing culture time range (5–12 h), the OD_{600} value of the RS2P mutant culture was always lower than the value of the wild-type culture, even though the initial OD_{600} value of the RS2P mutant culture was slightly higher (Supplementary Table S1). From 5 to 7 h, the OD_{600} value of the RS2P mutant culture was always approximately 10% lower than the OD_{600} value of the wild-type NisP culture. At the 8 h culture point, the OD_{600} value gap reached the maximal 19%, and the gap then gradually reduced. Because a lower OD_{600} value indicates fewer bacteria, the observed differences in the bacterial inhibition assay for the wild-type NisP and the RS2P mutant expression cultures may be caused by their different proliferation rates. Further experiments supported the hypothesis that when using the two cultures at the same OD_{600} for the bacterial inhibition assays, the resulting bacterial inhibition rings were of an approximately identical size at each OD_{600} point (Fig. 3*c*). Considering the only difference between the two strains is that one expresses wild-type NisP and the other expresses the NisP mutant with an irremovable C-terminus, we conclude that the C-terminal auto-cleavage activity of NisP does not affect the maturation of nisin but decreases the growth rate of *L. lactis*. Notably, the last 30 C-terminal residues of NisP can be characterized as a consensus LP*X*TG cell-wall binding motif that is found in many Gram-positive bacterial proteins (Fischetti *et al.*, 1990). Because the identified auto-cleavage site is at the N-terminus of the LP*X*TG motif, auto-cleavage should lead to release of NisP from the cell wall. Understanding of the detailed biological function of the C-terminal auto-cleavage of NisP will require further study and verification.

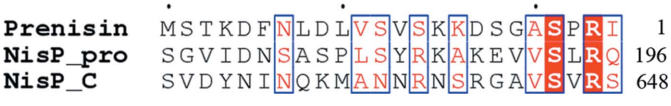

Figure 4
Sequence alignment of prenisin, NisP propeptide and residues near the NisP C-terminal cleavage site. Identical residues are highlighted with a red background and conserved residues are coloured red.

4. Discussion

It has been reported that calcium ions are essential to maintain the stability and activity of many proteases (Gros *et al.*, 1991). The number of potential calcium ion-binding sites in the members of the subtilase family can vary greatly (Tanaka *et al.*, 2007). There are two calcium-binding sties in the paradigm *Bacillus* subtilisins, a strong site from which removal of the metal results in unfolding and auto-destruction, and a weak one which can reversibly bind calcium (Voordouw *et al.*, 1976; Bryan *et al.*, 1992; Siezen *et al.*, 1991). However, neither of them was found in the NisP structure since no corresponding residues responsible for calcium chelation are present. Another medium-strength calcium-binding site was delineated in thermitase (Gros *et al.*, 1991), which was also predicted to be the only calcium-binding site in NisP (Siezen *et al.*, 1995). However, the residues Asp287, Glu290, Asp292, Thr294, Asn296 and Asp299, which were expected to be involved in calcium chelation, exhibit a linear conformation in the NisP structure (Supplementary Figs. S4*a* and S4*b*) and cannot form a metal-ion coordination system. Accordingly, no Ca atom was found in the NisP structure even with 10 m*M* $CaCl_2$ present in the crystallization buffer. Furthermore, neither treatment with 0.1 *M* EDTA nor stepwise addition of calcium (up to 0.1 *M*) has a significant effect on the enzyme activity (Supplementary Fig. S4*c*), which supports the hypothesis that NisP functions as a calcium-independent subtilase.

NisP has been discovered to have the ability to cleave both prenisin between Arg−1 and Ile1 to release the mature nisin and its own pro-peptide between residues Arg195 and Gln196 prior to maturation (van der Meer *et al.*, 1993; Plat *et al.*, 2011). In our current studies, another unexpected cleavage site between Arg647 and Ser648 located in the C-terminal region of NisP was identified from structural and biochemical data. To further identify the common substrate-recognition pattern of NisP, a sequence alignment of the cleavage-site residues from prenisin, the NisP propeptide and the NisP C-terminal region was performed (Fig. 4), which showed that the conserved arginine residue exclusively occupies the P1 position (the position before the cleavage site). Compared with the strong preference for Arg in the P1 position, a hydrophobic residue Ala in prenisin or Val in the NisP propeptide and C-terminal region was found at the P4 position, in line with a hydrophobic pocket in the NisP surface (Fig. 1*d*). Previous studies showed that substituting a glutamine for Arg−1 or an aspartate for Ala−4 in prenisin severely affects the cleavage of the leader peptide by NisP (van der Meer *et al.*, 1994). Based on the relevant binding environment identified in the NisP structure, the substitutions mentioned above will prevent the substrates from accessing the P1 and P4 positions,

leading to lower cleavage efficiency. In addition, in our structure the C-peptide residues in the P3 and P2 positions (Ser645 and Val646) form a small β-strand. However, in prenisin the P2 position is a proline residue that tends to disrupt such a secondary structure, hinting that the affinity of NisP for prenisin at the P2 position could be even lower than that at the two auto-cleavage sites. However, previous studies showed that NisP cleaves neither unmodified nor dehydrated prenisin (Kuipers *et al.*, 2004; Koponen *et al.*, 2002), suggesting that the thioether rings in prenisin provide additional interactions with NisP rather than the leader peptide discussed above. Our structure demonstrates how NisP recognizes the consensus sequence before the cleavage site, while the recognition mechanism for the thioether rings in prenisin requires further investigation.

The authors are grateful to Yu Guo for assistance with data collection, all of the beamline scientists at the Photon Factory in Japan for technical support, and Lixin Li for analysis of the mass spectrometry. This study was supported by the National Key Basic Research Program of China (973 Program; Grant Nos. 2014CB542800 and 2010CB833600), the Young Scientists Fund of the National Natural Science Foundation of China (Grant Nos. 31000345 and 31000056) and the Natural Science Foundation of Tianjin, China (Grant No. 09JCZDJC18000).

References

Adams, P. D. *et al.* (2010). *Acta Cryst.* D**66**, 213–221.
Berman, H. M., Westbrook, J., Feng, Z., Gilliland, G., Bhat, T. N., Weissig, H., Shindyalov, I. N. & Bourne, P. E. (2000). *Nucleic Acids Res.* **28**, 235–242.
Bryan, P., Alexander, P., Strausberg, S., Schwarz, F., Lan, W., Gilliland, G. & Gallagher, D. T. (1992). *Biochemistry*, **31**, 4937–4945.
Chen, V. B., Arendall, W. B., Headd, J. J., Keedy, D. A., Immormino, R. M., Kapral, G. J., Murray, L. W., Richardson, J. S. & Richardson, D. C. (2010). *Acta Cryst.* D**66**, 12–21.
Cunningham, D. F. & O'Connor, B. (1997). *Biochim. Biophys. Acta*, **1343**, 160–186.
Delves-Broughton, J. (1990). *Food Technol.* **44**, 110–117.
Delves-Broughton, J., Blackburn, P., Evans, R. J. & Hugenholtz, J. (1996). *Antonie Van Leeuwenhoek*, **69**, 193–202.
Dodson, G. & Wlodawer, A. (1998). *Trends Biochem. Sci.* **23**, 347–352.
Emsley, P., Lohkamp, B., Scott, W. G. & Cowtan, K. (2010). *Acta Cryst.* D**66**, 486–501.
Engh, R. A. & Huber, R. (1991). *Acta Cryst.* A**47**, 392–400.
Fischetti, V. A., Pancholi, V. & Schneewind, O. (1990). *Mol. Microbiol.* **4**, 1603–1605.
Germain, D., Dumas, F., Vernet, T., Bourbonnais, Y., Thomas, D. Y. & Boileau, G. (1992). *FEBS Lett.* **299**, 283–286.
Gros, P., Kalk, K. H. & Hol, W. G. J. (1991). *J. Biol. Chem.* **266**, 2953–2961.
Hurst, A. (1981). *Adv. Appl. Microbiol.* **27**, 85–123.
Koponen, O., Tolonen, M., Qiao, M., Wahlström, G., Helin, J. & Saris, P. E. J. (2002). *Microbiology*, **148**, 3561–3568.
Kuipers, O. P., Beerthuyzen, M. M., Siezen, R. J. & De Vos, W. M. (1993). *Eur. J. Biochem.* **216**, 281–291.
Kuipers, A., de Boef, E., Rink, R., Fekken, S., Kluskens, L. D., Driessen, A. J., Leenhouts, K., Kuipers, O. P. & Moll, G. N. (2004). *J. Biol. Chem.* **279**, 22176–22182.
Leduc, R., Molloy, S. S., Thorne, B. A. & Thomas, G. (1992). *J. Biol. Chem.* **267**, 14304–14308.
Li, H. & O'Sullivan, D. J. (2006). *J. Bacteriol.* **188**, 8496–8503.
Lubelski, J., Rink, R., Khusainov, R., Moll, G. N. & Kuipers, O. P. (2008). *Cell. Mol. Life Sci.* **65**, 455–476.
McAuliffe, O., Ross, R. P. & Hill, C. (2001). *FEMS Microbiol. Rev.* **25**, 285–308.
Meer, J. R. van der, Polman, J., Beerthuyzen, M. M., Siezen, R. J., Kuipers, O. P. & De Vos, W. M. (1993). *J. Bacteriol.* **175**, 2578–2588.
Meer, J. R. van der, Rollema, H. S., Siezen, R. J., Beerthuyzen, M. M., Kuipers, O. P. & de Vos, W. M. (1994). *J. Biol. Chem.* **269**, 3555–3562.
Murshudov, G. N., Skubák, P., Lebedev, A. A., Pannu, N. S., Steiner, R. A., Nicholls, R. A., Winn, M. D., Long, F. & Vagin, A. A. (2011). *Acta Cryst.* D**67**, 355–367.
Otwinowski, Z. & Minor, W. (1997). *Methods Enzymol.* **276**, 307–326.
Perrakis, A., Morris, R. & Lamzin, V. S. (1999). *Nature Struct. Biol.* **6**, 458–463.
Plat, A., Kluskens, L. D., Kuipers, A., Rink, R. & Moll, G. N. (2011). *Appl. Environ. Microbiol.* **77**, 604–611.
Polgar, L. (2005). *Cell. Mol. Life Sci.* **62**, 2161–2172.
Power, S. D., Adams, R. M. & Wells, J. A. (1986). *Proc. Natl Acad. Sci. USA*, **83**, 3096–3100.
Qiao, M., Ye, S., Koponen, O., Ra, R., Usabiaga, M., Immonen, T. & Saris, P. E. J. (1996). *J. Appl. Bacteriol.* **80**, 626–634.
Ra, S. R., Qiao, M., Immonen, T., Pujana, I. & Saris, P. E. J. (1996). *Microbiology*, **142**, 1281–1288.
Radisky, E. S. & Koshland, D. E. Jr (2002). *Proc. Natl Acad. Sci. USA*, **99**, 10316–10321.
Sahl, H. G. & Bierbaum, G. (1998). *Annu. Rev. Microbiol.* **52**, 41–79.
Siezen, R. J., de Vos, W. M., Leunissen, J. A. & Dijkstra, B. W. (1991). *Protein Eng.* **4**, 719–737.
Siezen, R. J., Rollema, H. S., Kuipers, O. P. & de Vos, W. M. (1995). *Protein Eng.* **8**, 117–125.
Tanaka, S., Saito, K., Chon, H., Matsumura, H., Koga, Y., Takano, K. & Kanaya, S. (2007). *J. Biol. Chem.* **282**, 8246–8255.
Voordouw, G., Milo, C. & Roche, R. S. (1976). *Biochemistry*, **15**, 3716–3724.
Winn, M. D. *et al.* (2011). *Acta Cryst.* D**67**, 235–242.
Xuanyuan, Z., Wu, Z., Li, R., Jiang, D., Su, J., Xu, H., Bai, Y., Zhang, X., Saris, P. E. J. & Qiao, M. (2010). *Curr. Microbiol.* **61**, 329–334.